Dual-Mode FMCW Harmonic Radar Supporting Auxiliary Transmitter Operation

Greg Storz
Greg Storz Consulting
Auckland, New Zealand
greg@storz.nz

Anastasia Lavrenko
Radio Systems group
University of Twente
Enschede, Netherlands
a.lavrenko@utwente.nl

James Cavers and Graeme Woodward
Wireless Research Centre
University of Canterbury
Christchurch, New Zealand
graeme.woodward@canterbury.ac.nz

***Abstract*—In this paper, we propose a dual-mode FMCW harmonic radar capable of both harmonic and intermodulation operation. The presented system prototype operates in the X-band in the uplink (radar to the target) and the K-band in the downlink (target to the radar). For intermodulation operation, an additional external X-band tone transmitter is utilized to boost the target response. The viability of the proposed system is demonstrated in field tests using a passive harmonic tag as a nonlinear target.**

***Index Terms*—nonlinear radar, harmonic radar, intermodulation radar, FMCW radar**

I. Introduction

Nonlinear radar is widely used for the detection and tracking of objects in highly cluttered environments [1]. In contrast to conventional radar systems that are designed for tracking of targets producing linear (around the same central frequency) response when illuminated with an RF signal, in nonlinear radar the target is nonlinear and it generates a return signal at a frequency different from that of the illuminating signal. This frequency separation between the transmit and receive signals enables suppression of linear clutter that stays predominantly at the transmit frequency. Such non-linear operation can be induced intentionally, e.g. by placing a non-linear tag on the target of interest [2], [3], as a by-product of other processes, such as corrosion in metals [4], or due to inherent parasitic non-linearities present in any electronic device [5], [6].

Depending on the implementation, nonlinear radar can be of several sub-varieties. The two most common ones are the harmonic and intermodulation radar. In harmonic radar (HR), the radar unit transmits a signal at some fundamental frequency f_0 and receives a signal return from a nonlinear target at a harmonic frequency nf_0 (where n is an integer). Since for most nonlinear targets the second harmonic output has the highest power, HR systems are typically designed to receive the return signal at $2f_0$. In intermodulation radar (IR), the nonlinear target is illuminated with two signal sources at two different frequencies f_1 and f_2 producing a signal return at $mf_1 \pm nf_2$ instead [5].

This work was partially supported by the NWO VENI Grant 19156, the Royal Society of New Zealand Catalyst:Seeding grant CSG-FRI1802 and the Endeavour Smart Idea grant UOCX2108 by the New Zealand MBIE.

Historically, nonlinear radar systems have been dominated by HR. A number of harmonic systems have been designed for different applications including insect tracking [7]–[9], electronic surveillance [10], [11], and search and rescue [12], [13]. In recent years, IR has begun to attract more attention as a potential alternative to harmonic operation. One of the challenges in HR is its increased requirements on receiver linearization [14], [15]. Utilizing mixing intermodulation product(s) instead of the harmonic one removes the problems associated with parasitic harmonic signal leakage from the transmitter to the receiver. It also provides more degrees of freedom for system design due to the added flexibility of choosing the frequency separation between the two signal sources and the mixing products to be processed at the receiver. For example, one can choose the transmit frequencies so that the transmitter and receiver operate in the same frequency band, which enables sharing of the antenna and some of the hardware. Following this principle, multitone IR systems were developed in [5], [16], [17] where at least two tone signals are transmitted from a single transceiver and then different order intermodulation products are detected at a collocated receiver. In [18], an IR system is proposed that uses a pseudo-random coded BPSK-modulated ranging pulse and a continuous tone signal. A second-order intermodulation product ($f_1 + f_2$) is then detected and processed at the receiver. An IR using frequency modulated continuous wave (FMCW) waveform was described in [19] and [20]. Both of these works applied the same basic approach as in [18], that is, using a double-branch transmitter that generates a ranging signal and a single tone, while the receiver is designed to receive and process an upper or lower third-order intermodulation product. The downside of only receiving the intermodulation products in nonlinear FMCW radar is a potential loss in resolution capabilities since in harmonic FMCW implementation the resolution is doubled by the squaring of the waveform [9]. Finally, [21] discusses using arbitrary noise-like waveforms to produce intermodulation response at the nonlinear target.

A somewhat different approach is suggested in [22], [23] where a ranging and a tone signal are transmitted from two different, spatially separated units. Namely, a ranging signal is transmitted from a radar transceiver module while a tone signal is produced by a so-called auxiliary helper transmitter. The

978-1-6654-8278-3/23/$31.00 ©2023 IEEE

radar module then processes the second-order intermodulation product produced by the tag. One advantage of having an auxiliary tone transmitter that is separated from the main radar module is that the two can be placed at different distances to the target. Since the helper only transmits an unmodulated carrier, it can be very compact and lightweight, allowing it to be portable and even placed on a mobile platform, for example, to be able to scan a larger area than with a single stationary radar module, as suggested by the results presented in [24]. Furthermore, multiple auxiliary helper transmitters can be used to increase the tag output and/or system coverage incrementally. Capitalising on this idea, in this paper, we present a novel dual-mode FMCW nonlinear radar system that combines the benefits of harmonic and intermodulation operation while accommodating the concept of auxiliary helper transmitter introduced in [22], [23]. The proposed system consists of an FMCW nonlinear radar unit comprised of a 9.3GHz transmitter producing a 80MHz chirp and a dual branch receiver designed to receive the harmonic signal return at 18.6GHz as well as the second order intermodulation signal at 18.8GHz. To produce the latter, a separate auxiliary transmitter is used that generates a tone at 9.5 GHz. Thus, the system can operate as a regular FMCW harmonic radar in the absence of the helper, or use both harmonic and intermodulation outputs when the helper is present.

II. Nonlinear Radar

A. Nonlinear response model

It is common to model the response of a generic nonlinear target as a following power series [5]

$$E_{\text{out}}(t) = \sum_{n=1}^{\infty} k_n E_{\text{in}}^n(t) = \sum_{n=1}^{\infty} E_n(t), \tag{1}$$

where $E_{\text{in}}(t)$, $E_{\text{out}}(t)$ are the incident and reflected electric fields, respectively, k_n are the power-series coefficients that depend on the target and $E_n(t) = k_n E_{\text{in}}^n(t)$. Consider now a passband input $E_{\text{in}}(t) = A\text{Re}\{s(t)e^{\jmath 2\pi f_c t}\}$, where $s(t)$ is an arbitrary complex baseband waveform, f_c is the central frequency, and A is the signal amplitude. Then one can show that the n-th power term in (1) can be written as

$$E_n(t) = k_n \sum_m h_{m,n} A^n \text{Re}\{s^m(t)|s(t)|^{n-m} e^{\jmath 2\pi m f_c t}\}, \tag{2}$$

where $m = 0, 2, \ldots n$ for even n and $m = 1, 3, \ldots, n$ for odd n, while $h_{m,n}$ is given by

$$h_{m,n} = \begin{cases} \dfrac{C_n^{n/2}}{2^n}, & \text{for } m = 0,\ n \text{ even} \\ \dfrac{C_n^{(n+m)/2}}{2^{n-1}}, & \text{otherwise} \end{cases} \tag{3}$$

in which $C_n^k = \frac{n!}{k!(n-k)!}$ is the binomial coefficient. Assuming for simplicity a constant unit magnitude waveform (e.g., a chirp or a polyphase sequence), (2) simplifies to

$$E_n(t) = k_n \sum_m h_{m,n} A^n \text{Re}\{s^m(t) e^{\jmath 2\pi m f_c t}\}. \tag{4}$$

The bandpass representation of $E_n(t)$ in (4) illustrates the harmonic composition of the nonlinear target response which contains components at mf_c. It also shows that for a polynomial non-linearity acting on a constant magnitude signal, all contributions at the harmonic with index m are proportional to the m-th power of the input (complex) waveform $s(t)$.

B. Harmonic radar

In HR, the radar transmitter emits an RF signal at the central frequency of f_0 and the receiver detects and processes a harmonic return at mf_0. Looking at (4) and (3) we can note that the amplitude of the harmonics decreases with m and therefore the second harmonic, being the strongest, is most commonly chosen for system design. It is clear from (4) that at a given even (odd) harmonic index m, there are contributions from all even (odd) powers $n \geq m$. However, at the low incident power, when the magnitude A is small, contributions from $n > m$ will have rapidly decreasing amplitudes, and the target response will be dominated by the $n = m$ term. Therefore, at low incident power characteristic of the target being close to the maximum range, the second-harmonic response boils down to

$$E_{\text{refl}}(t) = 0.5 k_2 A^2 \text{Re}\{s^2(t) e^{\jmath 2\pi 2 f_0 t}\}, \tag{5}$$

where k_2 depends on the target properties.

C. Intermodulation radar

In IR, a nonlinear target is illuminated by a linear combination of RF signals. Suppose that there are two incident signals with baseband complex envelopes $s_1(t)$, $s_2(t)$ and central frequencies f_1, f_2, respectively, where for clarity we consider $f_2 > f_1$. Then, $E_{\text{in}}(t) = E_{\text{in},1}(t) + E_{\text{in},2}(t)$, where $E_{\text{in},1}(t) = A_1 \text{Re}\{s_1(t)e^{\jmath 2\pi f_1 t}\}$ and $E_{\text{in},2}(t) = A_2 \text{Re}\{s_2(t)e^{\jmath 2\pi f_2 t}\}$, while the n-th power term in (1) becomes

$$E_n(t) = k_n \sum_{p=0}^{n} C_n^p E_{\text{in},1}^{n-p}(t) E_{\text{in},2}^p(t). \tag{6}$$

Let us now restrict our analysis to the second-order product only ($n = 2$). Using (4), it is easy to show that this yields the following output

$$\begin{aligned} E_{\text{refl}}(t) = 0.5 k_2 \Big(& A_1^2 \text{Re}\{s_1^2(t) e^{\jmath 2\pi 2 f_1 t}\} \\ & + A_2^2 \text{Re}\{s_2^2(t) e^{\jmath 2\pi 2 f_2 t}\} \\ & + 2A_1 A_2 \text{Re}\{s_1(t) s_2(t) e^{\jmath 2\pi (f_1 + f_2) t}\} \\ & + 2A_1 A_2 \text{Re}\{s_1(t) s_2^*(t) e^{\jmath 2\pi (f_2 - f_1) t}\} \Big), \end{aligned} \tag{7}$$

where $(\cdot)^*$ denotes complex conjugation. Eq. 7 shows that second-order nonlinearity produces four mixing products: two second harmonic outputs at $2f_1, 2f_2$ corresponding to the two individual incident signals as well as two intermodulation cross-products at $f_2 \pm f_1$. Similarly, higher-order products will produce intermodulation components at $m_1 f_1 \pm m_2 f_2$. Eq. 7 also suggests that when the amplitudes of the incident signals are equal, the second-order intermodulation products yield 6dB higher reflected power than the harmonic ones.

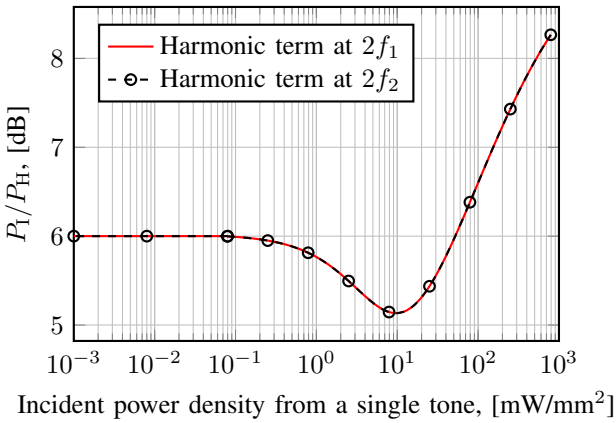

Fig. 1: Received power of the intermodulation term (P_{I}) relative to the received power of the harmonic terms (P_{H}) as a function of the power density incident on the nonlinear target.

Fig. 1 tests this prediction on an example of a two-tone input signal ($s_1(t) = s_2(t) = 1$). It shows the received power of the intermodulation term at $f_2 + f_1$ relative to the received power of the harmonic terms at $2f_1$,$2f_2$ measured using a spectrum analyser and a passive harmonic tag from [3] as a nonlinear target. The two input tones had a frequency separation of $f_2 - f_1 = 10$kHz and equal transmit power that was simultaneously swept so that the incident power density at the target from both tones was kept equal. We can observe that at low incident power levels the intermodulation term is 6dB larger, as predicted by (7). Increasing incident power density first results in a slight decrease of the relative power of the intermodulation term followed by its rapid increase. The former is due to the influence of higher-order terms not included in (7), while the latter rapid growth is likely due to the inadequacy of the power series model for larger incident power levels. Notwithstanding, Fig. 1 shows that irrespective of the incident power level the second-order intermodulation term has at least 5dB higher power than the harmonic ones.

III. Dual-mode FMCW Harmonic Radar Prototype

In this work, we propose a dual-mode FMCW harmonic radar that is capable of receiving both harmonic and intermodulation terms simultaneously. One of the biggest advantages of FMCW radar is that it achieves high range resolution and system sensitivity with low signal processing effort. Nonlinear operation also largely removes limitations on the receiver input level, as well as on the amplitude and phase noise of the transmitted signal that are typical for linear FMCW radar [9].

A. Nonlinear FMCW radar

In FMCW radar, the transmit waveform is a frequency chirp, as is schematically shown in Fig. 2a. Considering for simplicity a single chirp of duration T, in the bandpass notation of the previous section the corresponding waveform can be written as $s_1(t) = e^{j2\pi(\alpha t - 0.5B)t}$, where B is the chirp bandwidth and $\alpha = B/T$ is the chirp frequency sweep rate. From (5), in harmonic FMCW radar the return chirp is located at double the frequency and its baseband waveform is

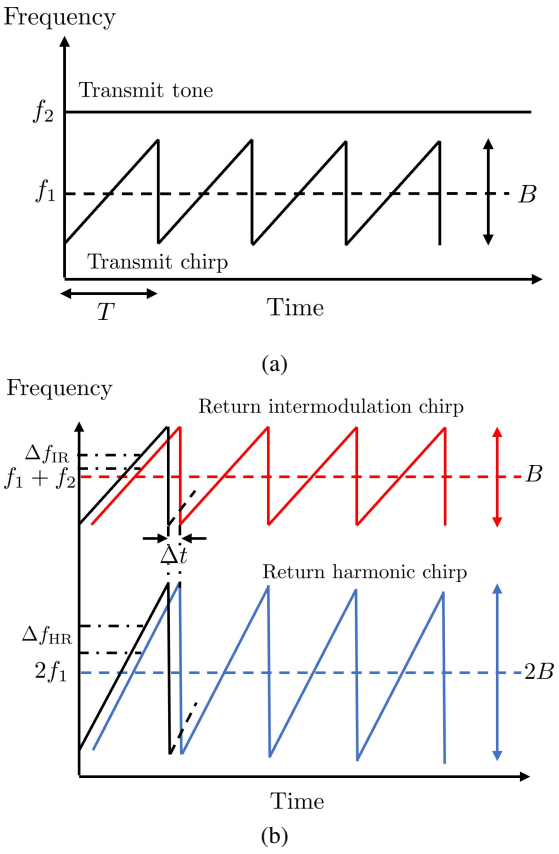

Fig. 2: Frequency composition of transmit (a) and return (b) signals in nonlinear FMCW radar.

$s_{\mathrm{HRx}}(t) = s_1^2(t-\Delta t) = e^{j2\pi 2(\alpha(t-\Delta t)-B)t}$ in which Δt is the time delay between the transmit and receive chirps. This shows that the return chirp in this case has double the bandwidth (see Fig. 2b) and hence the distance to the target can be determined as

$$R = \frac{c\Delta t}{2} = \frac{c\Delta f_{\mathrm{HR}}}{4\alpha}, \tag{8}$$

where c is the speed of light and Δf_{HR} is the frequency shift between the transmit and receive chirps, commonly referred to as the beat frequency. Due to the doubling of the chirp bandwidth, the resolution becomes $\delta_R = c/4B$.

In case of intermodulation FMCW radar where the second signal impinging on the nonlinear target is simply a tone at f_2, i.e., $s_2(t) = 1$, the return signal contains three chirps: the harmonic chirp with bandwidth $2B$ that is located at $2f_1$, and two intermodulation chirps of bandwidth B (one centered around $(f_1 + f_2)$ and the other at $(f_2 - f_1)$). All three waveforms are delayed by Δt. Note that to ensure that the components do not overlap, we also require that $f_2 > f_1 + 3B/2$. Processing any of these two intermodulation chirps one can compute the distance to the target as in regular (linear) FMCW radar, i.e.,

$$R = \frac{c\Delta t}{2} = \frac{c\Delta f_{\mathrm{IR}}}{2\alpha}, \tag{9}$$

The resolution in this case is also the same as in linear FMCW radar, namely $\delta_R = c/2B$.

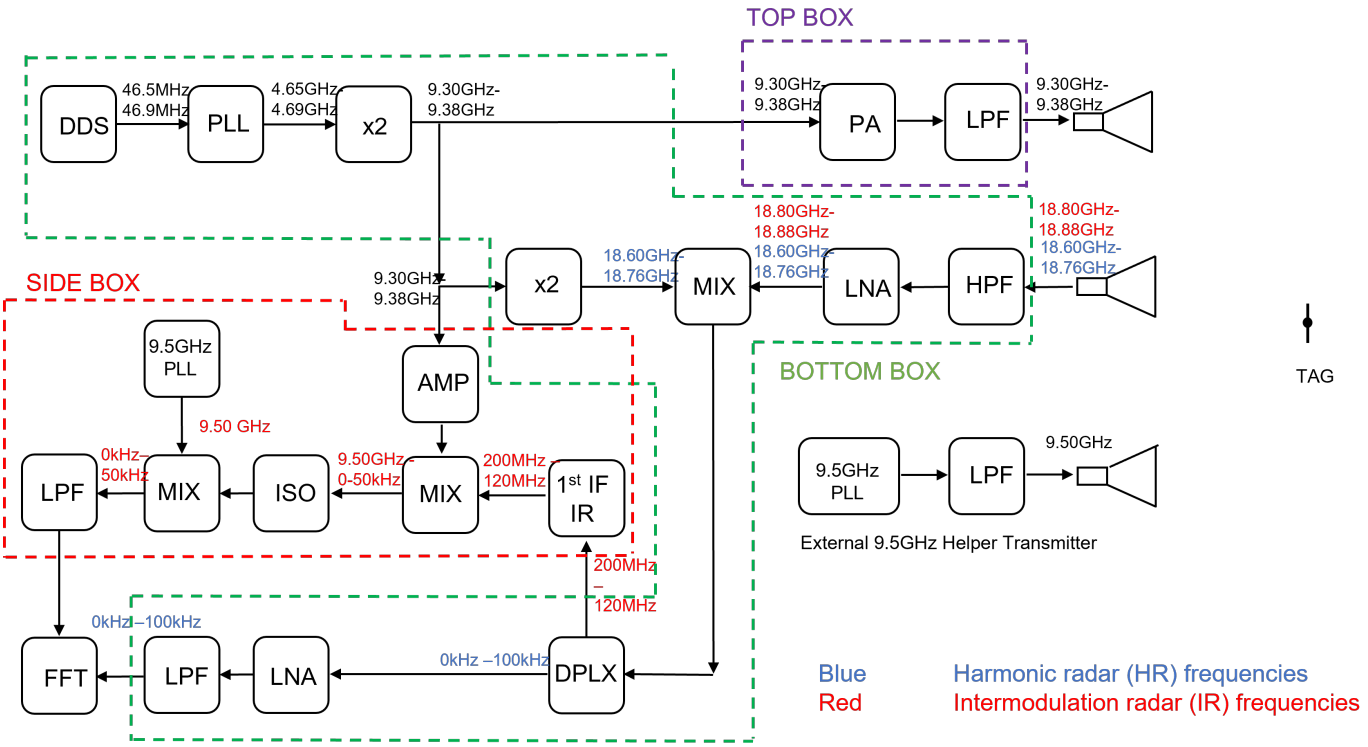

Fig. 3: Block diagram of the prototype 9.3/18.6 GHz dual-mode FMCW harmonic radar and an auxiliary helper transmitter operating at 9.5 GHz. The following abbreviations are used in the diagram: direct digital synthesis (DDS), phase locked loop (PLL), power amplifier (PA), low pass filter (LPF), high pass filter (HPF), low-noise amplifier (LNA), mixer (MIX), amplifier (AMP), diplexer (DPLX), intermediate frequency (IR), isolator (ISO), fast Fourier transform (FFT). The colored dashed boxes indicate which compartment the corresponding components are housed in in the test prototype shown in Fig. 4.

B. Dual-mode FMCW harmonic radar

Fig. 3 shows a block diagram of the proposed dual-mode FMCW harmonic radar prototype. The radar transceiver consists of a transmit module that generates an $B = 80$MHz chirp sweeping from 9.3GHz to 9.38GHz (so $f_1 = 9.34$GHz) and a double-branch receiver. To reduce power consumption, the radar was designed to operate at a 10% duty cycle with 1ms of sweep time and 9ms of off-time. To generate an intermodulation response from a nonlinear target, an additional external (helper) transmitter is utilized that produces a tone signal at $f_2 = 9.5$GHz. This results in a harmonic return chirp spanning $2B = 160$MHz from 18.60GHz to 18.76GHz (so $2f_2 = 18.68$GHz) and an $B = 80$MHz upper-band intermodulation chirp that goes from 18.80 to 18.88GHz (so $f_1 + f_2 = 18.84$GHz). This choice of frequencies ensures that the two chirps, the harmonic and the intermodulation one, are close enough in frequency to use the same receive antenna and be passed together to the intermediate frequency (IF), while have enough separation to be isolated at a later stage (see the non-overlap requirement discussed in the previous section).

In the receiver, the received signal containing both chirps is first mixed with the $18.60 - 18.76$GHz sweep signal from the transmitter's local oscillator (LO) and then passed to the diplexer. The diplexer separates the harmonic beat frequency output, which is now ready to be amplified, filtered and passed to the digitizer, and the signal containing the intermodulation output. The latter is now a mixture of the harmonic frequency sweep and the linear sweep, so additional down-conversion is required to extract the intermodulation beat frequency. This is done in two steps. First, the mixture signal is multiplied with the $9.30 - 9.38$GHz sweep signal from the transmitter's LO, which removes the linear sweep and moves the beat frequency output to 9.5GHz. In the second step, it is down-converted using additional 9.5GHz LO. Since there are two separate 9.5GHz LOs, one at the helper to generate the tone signal and one at the radar receiver to down-convert the intermodulation chirp, any frequency difference between them will directly contribute to an error in the estimated beat frequency. To bring the two closer together, the helper transmitter's LO is disciplined using GPS. The two beat frequency outputs are then passed to the two channels of a DIGILENT Analog Discovery 2TM USB oscilloscope for digitization and computation of the Fast Fourier Transform (FFT). Note that since this design is meant for operation at close range and we do not expect our target to be further away than 50m, we limit the beat frequency range to 100kHz and 50kHz for harmonic and intermodulation outputs, respectively.

IV. Experimental Verification

To verify our design, we performed a series of field tests using a passive harmonic tag as a nonlinear target. The tag, shown in Fig. 4, consisted of a planar dipole with a MA4E2503L low barrier diode soldered across its feed point

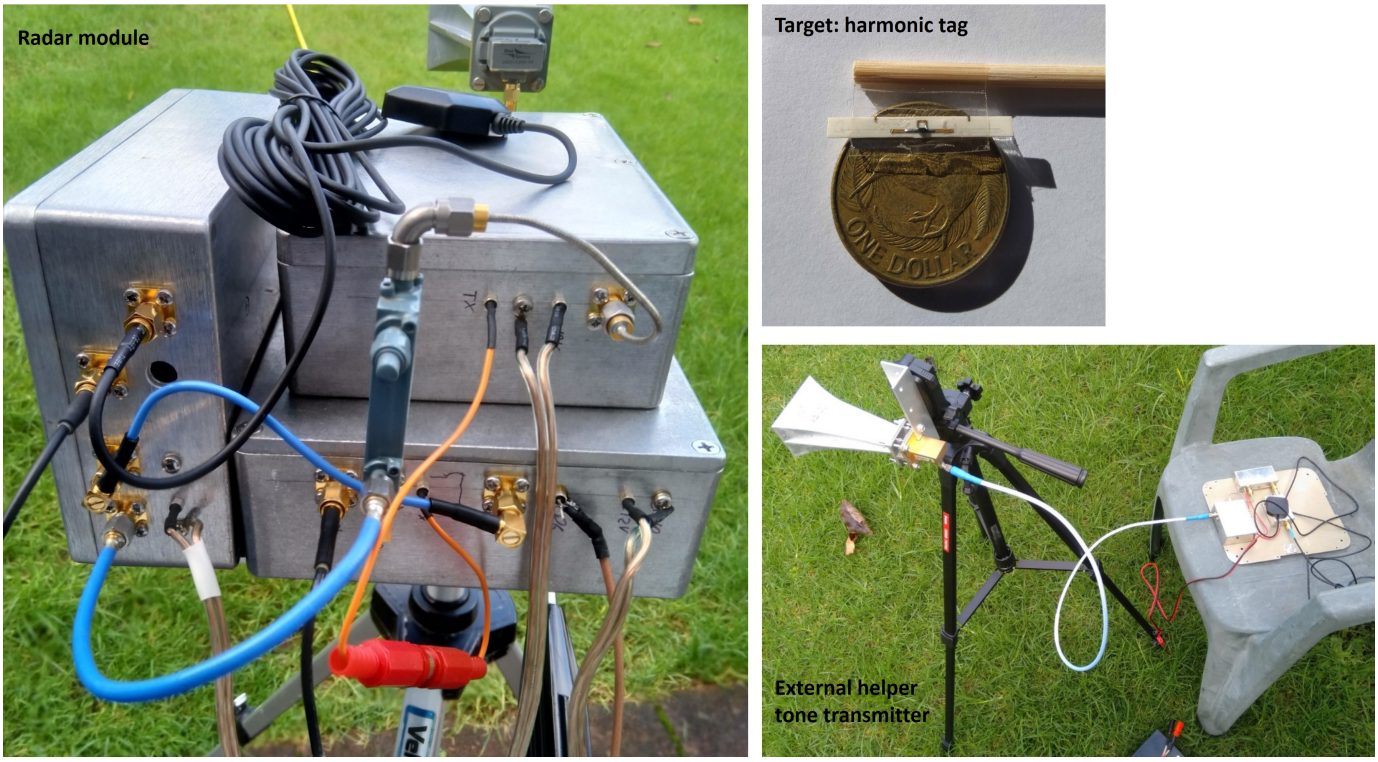

Fig. 4: Prototype 9.3/18.6 GHz dual-mode FMCW harmonic radar (left-hand side), passive harmonic tag (top right-hand side), and an auxiliary helper transmitter with GPSDO emitting an unmodulated carrier at 9.5 GHz (bottom right-hand side).

and a small inductive loop. It was positioned at distances d_1, d_2 to the radar module and the helper transmitter, respectively. The radar module was equipped with 15dBi transmit and receive horn antennas and had a transmit power of 10W. The helper tone transmitter also had a 15dBi horn antenna and produced a continuous tone signal with output power of 2W.

First, we tested how well the two 9.5GHz LOs (one at the helper transmitter and one at the radar receiver) are aligned in frequency. We measured the frequency separation between the two LOs coupled over the air which showed that they are disciplined within 40Hz of each other. This will yield approximately 13cm of range estimation error which is well within the range resolution bin for both outputs. Next, we performed field testing of harmonic and intermodulation operation with the passive harmonic tag from Fig. 4 as the nonlinear target. Fig. 5 shows harmonic and intermodulation beat frequencies for a tag positioned at $d_1 = 12$m to the radar module and two different distances to the helper transmitter: helper located at $d_2 = d_1 = 12$m (Fig. 5a) and $d_2 = 1$m (Fig. 5b). First, we note that in both cases we can clearly observe distinct peaks in the beat frequency of both harmonic and intermodulation outputs. For harmonic output, the peak corresponds to 11.5kHz, whereas for the intermodulation output it is located at 5.5kHz. As expected, the harmonic peak is at twice the frequency of the intermodulation peak, which both correspond to $R = 12$m. Note that the transmit power of the helper tone transmitter is 5 times lower that that of the radar module. At equal distances to the tag, this results in 5 times lower power density of the tone signal impinging on the target compared to the FMCW one. Nevertheless, at $d_1 = d_2$ the intermodulation peak is close to 20dB above the noise level[1] whereas the harmonic peak is just approximately 10dB above the noise. This clearly exceeds what (7) alone promises, which indicates additional improvement offered by the intermodulation operation in terms of the hardware implementation. As expected, moving the helper closer to the tag yields an increase of the intermodulation peak. This increase (about 14dB) however is smaller than what one would expect from a 12-fold distance decrease. One possible explanation is that at such close distance the tag was already in a saturation zone where the power-series model (1) is not representative of its behaviour. In conclusion, while our tests clearly demonstrate the validity of the proposed design, further investigations are required to fully quantify its performance.

REFERENCES

[1] A. Mishra and C. Li, "A review: Recent progress in the design and development of nonlinear radars," *Remote Sensing*, vol. 13, no. 24, pp. 4982, 2021.

[2] B. G Colpitts and G. Boiteau, "Harmonic radar transceiver design: miniature tags for insect tracking," *IEEE Transactions on Antennas and Propagation*, vol. 52, no. 11, pp. 2825–2832, 2004.

[3] A. Lavrenko, B. Litchfield, G. Woodward, and S. Pawson, "Design and evaluation of a compact harmonic transponder for insect tracking," *IEEE Microwave and Wireless Components Letters*, vol. 30, no. 4, pp. 445–448, 2020.

[4] V V Bereka, V V Rudenko, O V Zayets, and O M Pastushenko, "Radar method for the remote monitoring of the corrosion state of reinforced-concrete structures," *Materials Science*, pp. 1–7, 2022.

[1]Since the values displayed on the y axis depend on the receiver gain settings, a fair comparison necessitates consideration of signal to noise ratios rather than exact peak values.

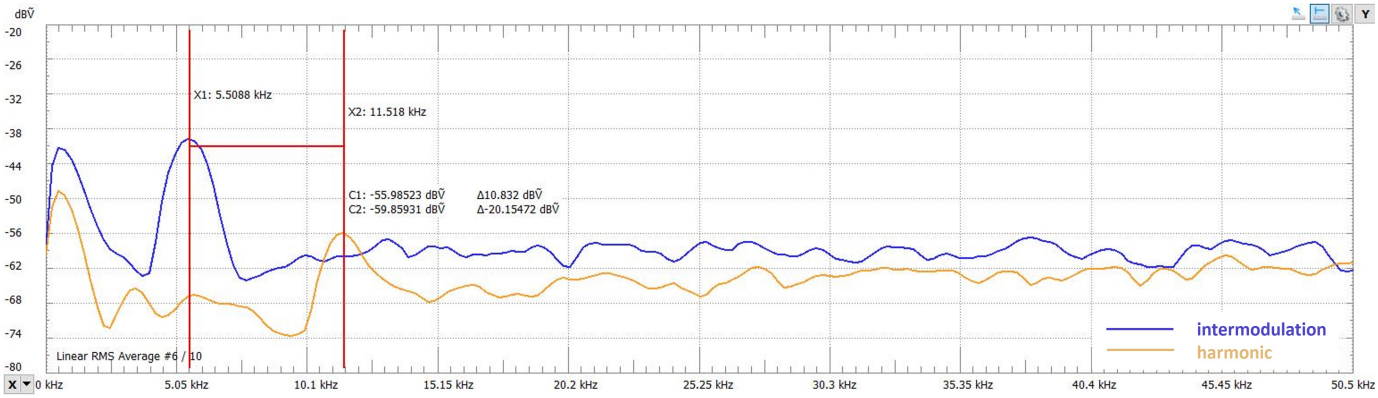

(a) Helper transmitter at $d_2 = 12$m

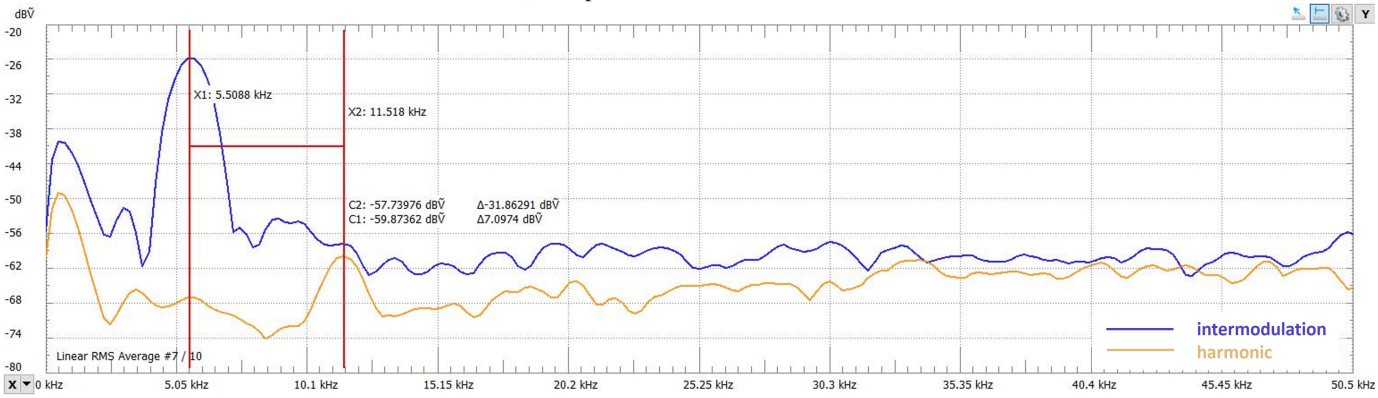

(b) Helper transmitter at $d_2 = 1$m

Fig. 5: Harmonic (blue line) and intermodulation (yellow line) beat frequency for a tag positioned at $d_1 = 12$m to the radar module. The helper transmitter was positioned at $d_2 = 12$m (a) and $d_2 = 1$m (b) to the tag.

[5] G. J Mazzaro, A. F Martone, and D. M McNamara, "Detection of RF electronics by multitone harmonic radar," *IEEE Transactions on Aerospace and Electronic Systems*, vol. 50, no. 1, pp. 477–490, 2014.

[6] A. Martorell, J. Raoult, L. Chusseau, and C. Carel, "Compact intermodulation radar for finding RF receivers," in *2019 16th European Radar Conference (EuRAD)*, 2019, pp. 109–112.

[7] J. R Riley and A. D Smith, "Design considerations for an harmonic radar to investigate the flight of insects at low altitude," *Computers and Electronics in Agriculture*, vol. 35, no. 2-3, pp. 151–169, 2002.

[8] R. Maggiora, M. Saccani, D. Milanesio, and M. Porporato, "An innovative harmonic radar to track flying insects: The case of vespa velutina," *Scientific reports*, vol. 9, no. 1, pp. 1–10, 2019.

[9] G. Storz and A. Lavrenko, "Compact low-cost FMCW harmonic radar for short range insect tracking," in *2020 IEEE International Radar Conference*, 2020, pp. 642–647.

[10] H. Aniktar, D. Baran, E. Karav, E. Akkaya, Y S. Birecik, and M. Sezgin, "Getting the bugs out: A portable harmonic radar system for electronic countersurveillance applications," *IEEE Microwave Magazine*, vol. 16, no. 10, pp. 40–52, 2015.

[11] B. Perez, G. Mazzaro, T. J Pierson, and D. Kotz, "Detecting the presence of electronic devices in smart homes using harmonic radar technology," *Remote Sensing*, vol. 14, no. 2, pp. 327, 2022.

[12] J. Olofsson, T. Forssén, G. Hendeby, I. Skog, and F. Gustafsson, "UAS-supported digitalized search-and-rescue using harmonic radar reflection," in *2020 IEEE Aerospace Conference*, 2020, pp. 1–7.

[13] T. Harzheim, M. Mühmel, and H. Heuermann, "A SFCW harmonic radar system for maritime search and rescue using passive and active tags," *International Journal of Microwave and Wireless Technologies*, vol. 13, no. 7, pp. 691–707, 2021.

[14] K. A Gallagher, R. M Narayanan, G. J Mazzaro, and K. D Sherbondy, "Linearization of a harmonic radar transmitter by feed-forward filter reflection," in *2014 Radar Conference*, 2014, pp. 1363–1368.

[15] A. Lavrenko, G. Woodward, and S. Pawson, "Parasitic harmonic cancellation for reliable tag detection with pulsed harmonic radar," in *2019 Radar Conference*, 2019, pp. 1–6.

[16] A. Mishra and C. Li, "A low power 5.8-GHz ISM-band intermodulation radar system for target motion discrimination," *IEEE Sensors Journal*, vol. 19, no. 20, pp. 9206–9214, 2019.

[17] H. Aniktar and D. Baran, "An efficient implementation of intermodulation radar with an integrated EMI sensor," *IEEE Sensors Journal*, vol. 21, no. 20, pp. 23492–23497, 2021.

[18] M.-L. Hsu, T.-H. Liu, T.-C. Yang, H.-C. Jhan, H. Wang, F.-R. Chang, K.-Y. Lin, E.-C. Yang, and Z.-M. Tsai, "Bee searching radar with high transmit–receive isolation using pulse pseudorandom code," *IEEE Transactions on Microwave Theory and Techniques*, vol. 64, no. 12, pp. 4324–4335, 2016.

[19] Z. Peng and C. Li, "Intermodulation FMCW (IM-FMCW) radar for nonlinear wearable targets detection," in *2018 United States National Committee of URSI National Radio Science Meeting (USNC-URSI NRSM)*, 2018, pp. 1–2.

[20] A. Mishra, J. Wang, D. Rodriguez, and C. Li, "Utilizing passive intermodulation response of frequency-modulated continuous-wave signal for target identification and mapping," *IEEE Sensors Journal*, vol. 21, no. 16, pp. 17817–17826, 2021.

[21] J. Owen, S. D Blunt, K. Gallagher, P. McCormick, C. Allen, and K. Sherbondy, "Nonlinear radar via intermodulation of FM noise waveform pairs," in *2018 IEEE Radar Conference*. IEEE, 2018, pp. 0951–0956.

[22] A. Lavrenko, S. Pawson, and J. Cavers, "On the use of additional transmitters for increasing detection range in harmonic radar," in *2019 13th International Conference on Signal Processing and Communication Systems (ICSPCS)*, 2019, pp. 1–8.

[23] A. Lavrenko, J.K Cavers, and G. K Woodward, "Harmonic radar with adaptively phase-coherent auxiliary transmitters," *IEEE Transactions on Signal Processing*, vol. 70, pp. 1788–1802, 2022.

[24] A. Lavrenko, "Effects of bistatic operation in harmonic radar," in *2022 19th European Radar Conference (EuRAD)*. IEEE, 2022, pp. 1–4.